HIFAN 1539
LBNL-61683

Simulating Electron Clouds in High-Current Ion Accelerators with Solenoid Focusing*

W. M. Sharp, D. P. Grote, R. H. Cohen, A. Friedman Lawrence Livermore National Laboratory
J.-L. Vay, P. A. Seidl, P. K. Roy, J. E. Coleman, J. Armijo Lawrence Berkeley National Laboratory
I. Haber *University of Maryland, College Park*

abstract

Contamination from electrons is a concern for the solenoid-focused ion accelerators being developed for experiments in high-energy-density physics (HEDP). These electrons are produced directly by beam ions hitting lattice elements and intercepting disgnostics, or indirectly by ionization of desorbed neutral gas, and they are believed responsible for time dependence of the beam radius, emittance, and focal distance seen on the Solenoid Transport Experiment (STX) at Lawrence Berkeley National Laboratory. The electrostatic particle-in-cell code WARP has been upgraded to included the physics needed to simulate electron-cloud phenomena. We present preliminary self-consistent simulations of STX experiments suggesting that the observed time dependence of the beam stems from a complicated interaction of beam ions, desorbed neutrals, and electrons.

1. Introduction

The Solenoid Transport Experiment (STX) is a scaled experiment to study emittance and envelope characteristics of a space-charge-dominated ion beam confined transversely by solenoids [1]. An important aspect of this project is determining how the beam transverse emittance and envelope parameters evolve during solenoid transport, and how these parameters are affected by stray electrons in the system. The expectation is that a comparison of STX results with findings from the High-Current Experiment (HCX) will guide the choice of the transport lattice for projected experiments in High-Energy Density Physics (HEDP) and Heavy-Ion Fusion (HIF).

The STX is presently undergoing commissioning, with two of the planned four solenoids being tested. The remaining solenoids will be added during the remainder of FY2006. The two-solenoid layout consists of a 300 kV diode producing a K^+ beam with a 0.3 mm-mrad emittance, a pair of 2.5-T solenoids, each 51.1 cm in length and separated by 8.9 cm, and last, a box with intercepting diagnostics to characterize the beam. Negatively biased rings or "traps" are situated at both ends of the solenoids to restrict electron movement toward the source, and an aperture plate may be inserted midway along the upstream trap to reduce beam current by about half. To date, the beam has been characterized by placing the diagnostics box in three locations: (1) immediately after the aperture and first electron trap, without the solenoids in place, (2) immediately after the second solenoid, with the second electron trap placed partly inside the last solenoid, and (3) 29 cm beyond the last solenoid.

Characterization of the beam in the first configuration, without solenoids and with a 1-cm-radius aperture plate in place, shows a 25 mA flattop of the beam that continues for about 10 μs, and slit-plate scans verify that the transverse emittance is about 14 mm-mrad. With the aperture removed, the current is 45 mA, and the emittance, 22 mm-mrad. A diagnostic measurement that is used repeatedly in the work reported here is the current from the final electron trap to ground through a 50-Ω resistor when a slit plate intercepts the beam 5-10 mm beyond the trap. The trap current in the case without solenoids is exactly what is expected. There is an initial positive current pulse of about 50 mA, balancing the image charge as the beam head enters the electron trap, followed by a gradually increasing positive current and finally a second capacitive pulse as the beam tail leaves the trap. The

increasing positive current as the beam midsection traverses the trap is due to neutrals that are desorbed from the plate, ionized by the beam, and attracted by the negative trap bias, typically -3 kV in these experiments. The second layout, with two solenoids followed immediately by diagnostics, has a strikingly different signature. After the first capacitive pulse and about 1 μs of rising positive current, the current develops high-frequency oscillations with a period of a few ns, shown in Fig. 1a. These oscillations can be delayed by adjusting the bias but not eliminated. Coinciding with the oscillations, a decrease in the beam radius was measured, the beam envelope switched at about 4 μs from converging to diverging. Moving the diagnostics and final trap downstream in the third layout eliminats the oscillations.

In this paper, we present results of the first STX simulations that include the interaction of the beam with the diagnostics and incorporate all the physical effects expected to be important. We briefly review the pertinent physics models in the computer code WARP used here and then compare simulations results with experimental data for the three STX layouts that have been studied to date, focusing on the cause of the oscillating trap current seen for the second layout. The findings are summarized in a concluding section, and the direction of future numerical work is briefly discussed.

2. Method

The electrostatic particle-in-cell code WARP [2] has recently been upgraded to handle multiple species and to model such species interactions as gas desorption, collisional ionization, and release of electrons from walls [3]. Primary and secondary electron production at walls is managed by the POSINST electron-cloud package [4], while impact ionization is handled by the txPhysics library [5]. An additional module handles desorption of neutrals [6]. Electrons are advanced with a time step that is one fifth that of heavier species, and a "drift-Lorentz" electron-advance algorithm [7] allows their gyrofrequency to be ignored when choosing a time step. In addition, the Chombo mesh-refinement code [8] is incorporated into WARP but is not used in the simulations reported here. Various other physical processes, such as recombination, charge exchange, ionization of background gas, and angular scattering, are not yet modeled by WARP but are expected to be inconsequential here.

A principal complication in using the new species interaction packages is the fact that desorption coefficients and collisional-ionization cross sections are not well known for singly charged heavy ions. For the simulations here, we assume that each ion striking a wall at normal incidence desorbs 10^4 neutrals, although simulations of HCX indicate that this value may be low by as much as a factor of three. The desorbed neutral species are also not known. Sample simulations using water and CO_2 indicate, however, that the dominate species must be substantially lighter. In the simulations here, we specify H_2 both because the calculated time for a positive current to appear on the electron trap is about what is observed on STX and because stainless steel is known to preferentially absorb hydrogen.

At present, WARP uses a very simple model to estimate impact-ionization cross sections [9], although the user may specify alternate values. In all the work here, we use a cross section of $5\text{x}10^{-20}$ m^2 for ionization of H_2 by 300 keV K^+. We note, however, that more sophisticated models [10, 11] as well as recent measurements [12] indicate that this value may be a factor of about five too large. Other impact-ionization processes, such as beam stripping, are included but appear to have little consequence.

In all the simulations reported here, the beam is modeled from the source to an intercepting slit plate in the diagnostics package. The beam is generated at the thermionic source using a well-tested Child-Langmuir algorithm and transported through a 4.6-cm-radius beam pipe, focused by fields calculated for ideal solenoids with longitudinal variation only. The lattice alignment, the solenoid fields, and the emitting surface are all assumed to be perfect, and eddy currents in metal plates near the lattice are ignored.

3. Results

3.1. No solenoids

WARP results for the first STX layout are in good agreement with the limited available data. Data was recorded for a single configuration, with the aperture plate placed between halves of the first electron trap and followed immediately by the diagnostics box. The WARP simulation shows a transverse emittance at the slit plate of 12 mm-mrd, compared with the measured value 14 mm-mrad, and the calculated edge radius is 1.2 cm, about 1 mm smaller than the measured value. Like the STX data, the simulation results show a capacitive spike as the beam enters the second half of the trap, followed by a gradually rising positive current until the simulation ends at 5 μs. Plots of the particles and charge densities show that a slowly evolving pattern develops soon after the beam reaches the intercepting slit plate. Primary and secondary electrons produced at the aperture and slit plate are confined near the plates by the negative trap bias, while those desorbed H_2 molecules that are ionized by the beam form well-defined streams from the plates to the halves of the adjacent electron trap. Over time, the electron layers at the plates become denser, the un-ionized H_2 spreads out, and the ion current to the plates increases. Little change is seen in beam parameters during the simulation. The main observable differences between the experiment and the simulation are a lower-amplitude and longer-duration capacitive pulse in the WARP results, indicating a slower rise time, and a larger electron-trap current, about 40 mA after 5 μs for WARP versus about 35 mA in the STX data.

3.2. Two solenoids and nearby diagnostics

WARP results for the second STX layout suggest a mechanism for the observed high-frequency oscillations in electron-trap current. The calculated electron-trap current, shown in Fig. 1b, shows features that resemble STX data in Fig. 1a. After the capacitive pulse, current is seen to rise slightly, due to ionized H_2 migrating to the trap. The H_2^+ density in front of the slit plate increases during this period, and we see the first evidence of an electron-ion instability. Positive fluctuation in the electrostatic potential near the plate attract upstream electrons. Some of

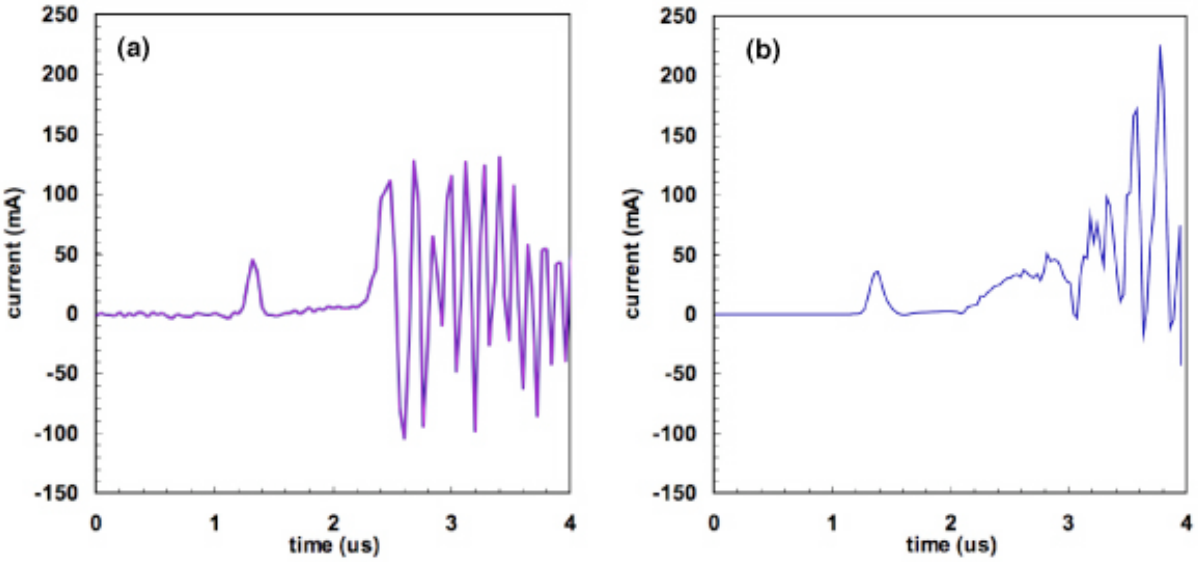

Fig. 1. Current from final electron trap to ground through a 50 resistor for two-solenoid STX layout with diagnostics immediately following the magnets: (a) Eperimental data and (b) WARP simulation.

these hit the plate and generate enough secondary electrons to reverse the potential, pushing some electrons through the negative trap potential. Since the ion density is high enough to shield the trap potential, this situation is akin to an oscillating virtual cathode [13]. After about 2.2 μs, current rises more steeply, a result both of electron release from impinging H_2^+ ions and of an increasing current of back-streaming secondary electrons from the slit plate. The oscillation amplitude builds up as the layer of H_2^+ ions lengthens and reaches a peak when the ions fill the electron trap. There are sufficient electrons in the solenoid fields after about 3 μs to affect the beam edge radius at the slit plate, so we see a gradual decrease until a minimum reached around 4 μs. After that the beam at the plate is diverging, and the radius begins to increase. There are clear differences between the experiment and this WARP calculation, notably the suddenness that the oscillations appear and their frequency, but we believe that this mechanism seen in the simulation is qualitatively correct.

A series of WARP runs shows that the trap-current oscillation is insensitive to the trap bias over the range -2 kV to -4kV but is suppressed by a greater negative bias voltages. The experiment, however, shows a more complicated dependence on the bias voltage. Oscillations are observed at -2 kV, -3 kV, and -4 kV, but are delayed by nearly 8 μs for a -2.5 kV bias. We have yet to develop a theoretical understanding of this observation.

The differences between theory and experiment suggest that some of the modeling choices are incorrect. As mentioned, there is evidence that the values chosen for desorption and ionization cross sections inaccurate, and we expect that the ionized H_2 is some mix of H^+ and H_2^+, rather than purely H_2^+. In addition, examination of data on the radial grid and on sequential ion time steps indicates that both the spatial gridding and the time step are too large to resolve the virtual cathode dynamics.

3.3. Two solenoids and remote diagnostics

The third STX layout was proposed by the experimental team to reduce the beam degradation seen with the second layout. An empty diagnostics box was inserted after the solenoids, adding 29 cm to the overall length, and the final electron trap was inserted through a hole between the grounded diagnostics boxes. As in the second layout, the slit plate is placed 9 mm beyond the end of the trap. This relocation of diagnostics farther downstream largely eliminates the problems for the 10-μs pulse duration. Beam envelope parameters remain nearly constant along the beam midsection, and no oscillations appear in the electron-trap current.

These experimental findings controvert WARP simulations of this case. The calculated behavior of all the species is qualitatively the same as for the second layout, with an additional time-of-flight delay and a slightly larger H_2^+ current to the electron trap being the main quantitative differences. This clear distinction between theory and experiment underlines to need to refine and benchmark the WARP physics models.

4. Conclusions

The WARP simulations of STX presented here are at best preliminary due to the uncertainty of critical physical parameters and the use of what we now believe are inadequate spatial and temporal resolution near the experimental diagnostics. Nonetheless, the simulations appear to demonstrate phenomena that match qualitatively what is seen in STX results. If the high-frequency oscillation of the electron-trap current is found in fact to result from the interaction of secondary electrons with ionized hydrogen from the slit plate, as discussed in Sec. 3.3, then there are several possible remedies. Moving the diagnostics farther from last solenoid has been shown recently to succeed, despite WARP simulations to the contrary. Another proposed solution is to place rings between solenoids biased so as to establish a negatively directed electric field along the axis of the lattice to expel electrons. This method will be tried with the four-solenoid configuration. A third approach is to replace the stainless-steel diagnostic apparatus with copper, which adsorbs far less hydrogen than stainless steel [14].

Future STX modeling will use the mesh-refinement routines in WARP to provide sufficient resolution of the virtual-cathode region seen near the slit plate. The time-resolution concern is reduced by this choice because the time step for each species is adjusted automatically to satisfy the particle Courant condition. We also plan to test the cross sections for collisional ionization recently measured at LBNL [12] and compare these with calculated values from recent analytic models [10, 11]. We anticipate that these changes will reduce or remove the large discrepancies now seen between STX simulations and the experimental results.

Acknowledgments

This work was performed under the auspices of the US Department of Energy by the University of California Lawrence Livermore and Lawrence Berkeley National Laboratories under contracts W-7405-Eng-48 and DE-AC03-76SF00098.

References

[1] P. A. Seidl, *et al.,* "Plans for Longitudinal and Transverse Neutralized Beam Compression Experiments and Initial Results from Solenoid Transport," in these proceedings (2006).
[2] D. P. Grote, A. Friedman, I. Haber, W. Fawley, and J.-L. Vay, Nucl. Instrum. Methods Phys. Res. A **415**, 428 (1998).
[3] J.-L. Vay, "New simulation capabilities of electron clouds in ion beams with large tune depression," in these proceedings (2006).
[4] M. A. Furman and M. Pivi, *Phys. Rev. ST Accel. Beams* **5,** 124404 (2002).
[5] See http://www.txcorp.com/technologies/TxPhysics/.
[6] J.-L. Vay, *et al.*, "Initial Self-Consistent 3-D Electron-Clouod Simulations of the LHC Beam with the Code WARP+POSINST," Proceedings of the 21st Particle Accelerator Conference, 16-20 May 2005, Knoxville, TN, p. 1479 (2006).
[7] R. H. Cohen, *et al..*, *Phys. Plasmas* **12**, 056708 (2005).
[8] J.-L. Vay, *et al., Phys. Plasmas* **11**, 5, 2928 (2004).
[9] S. P. Slinker, R. D. Taylor, and A. W. Ali, *J. Appl. Phys.* **63**, 1 (1988).
[10] M. S. Armel, PhD Thesis (2002).
[11] I. D. Kaganovich, E. Startsev, and R. C. Davidson, "Scaling and formulary of cross sections for ion-atom impact ionization," *New J. Physics*, to be published.
[12] M. Kireeff Covo, *et al.,* "Beam Interaction Measurements with a Retarding Field Analyzer," in these proceedings.
[13] W. Jiang and Magne Kristiansen, *Phys. Plasmas* **8**, 3781 (2001).
[14] L. R. Grisham, private communication.